

Hermes results on 3D imaging of the nucleon

L. L. Pappalardo^{*†}

Dipartimento di Fisica e Scienze della Terra, Università degli Studi di Ferrara and INFN

Sezione di Ferrara, Via Saragat 1, 44122 Ferrara, Italy

E-mail: pappalardo@fe.infn.it

The study of the quantum phase-space distribution of quarks and gluons inside nucleons in terms of TMDs and GPDs has become, in the last decade, a cutting-edge research field in hadron physics. These non-perturbative objects, respectively measurable in semi-inclusive deep-inelastic scattering and hard exclusive processes, allow to obtain 3-dimensional representations of the nucleon in the momentum and spatial coordinates as well as indirect insights into the still unknown parton orbital angular momentum. The HERMES experiment at HERA has been a precursor in this field. A selection of HERMES results sensitive to both TMDs and GPDs is presented.

*The 8th International Workshop on Chiral Dynamics, CD2015 ****

29 June 2015 - 03 July 2015

Pisa, Italy

^{*}Speaker.

[†]On behalf of the HERMES Collaboration

1. Introduction

Theoretical developments of the *parton model* in the framework of non-perturbative QCD followed by decades of deep-inelastic scattering (DIS) experiments have led to a relatively detailed description of the internal structure of nucleons in terms of quark and gluon degrees of freedom. In particular, very high-precision results on the longitudinal¹ momentum distribution of quarks, described by the spin-independent parton distribution function (PDF) $f_1(x)$, are provided by global fits of world data [1] that span several orders of magnitude in x and Q^2 , the longitudinal momentum fraction of the nucleon carried by the partons and the squared four-momentum transfer of the hard probe to the struck quark, respectively. In the last decades an increasing focus was put on the spin degrees of freedom of quarks and gluons, described by the spin-dependent *helicity* PDF $g_1(x)$. While a relatively precise knowledge of g_1 has been achieved for the valence quarks, large uncertainties still affect the results for sea quarks and gluons [1]. More recently, the HERMES experiment, followed by other experiments, provided first evidences of a non-zero transverse spin distribution of quarks in a transversely polarized nucleon. This distribution, described by the *transversity* PDF $h_1(x)$, is chiral-odd, and therefore can not be measured in inclusive DIS. It can be accessed in more complex processes, such as semi-inclusive DIS (SIDIS) or Drell-Yan, that involve another chiral-odd object. The three fundamental PDFs $f_1(x)$, $g_1(x)$ and $h_1(x)$ are said to be *collinear*, in the sense that they neglect any parton transverse momentum degree of freedom², thus providing 1-dimensional descriptions of the nucleon structure in terms of the longitudinal momentum fraction x .

In recent years, huge efforts are being focused towards a more comprehensive multi-dimensional description of the nucleon. The final goal is to map the full quantum phase-space distribution of quarks and gluons inside the nucleon, as formally encoded by the Wigner function. The latter, depending on both spatial and momentum coordinates of partons, represents the maximal knowledge on the partonic structure of nucleons. Since, due to the uncertainty principle, the Wigner function is not directly measurable, the main focus of present and future experiments in this field is on two independent classes of partially integrated objects, the Transverse Momentum Dependent PDFs (TMDs) and the Generalized Parton Distributions (GPDs). They allow for complementary descriptions of the nucleon in three dimensions (*nucleon tomography*), spanned by the quark's longitudinal momentum and, respectively, by its transverse momentum components and transverse spatial coordinates. Furthermore, they provide complementary insights into the yet unmeasured quark orbital angular momentum. Experimentally, TMDs and GPDs can be accessed through the analysis of specific azimuthal asymmetries measured, respectively, in SIDIS and hard exclusive processes, such as hard lepto-production of real photons or mesons.

2. Transverse Momentum Distributions

At leading-twist, eight TMDs, each with a specific probabilistic interpretation in terms of quark number densities, enter the SIDIS cross-section in conjunction with a fragmentation func-

¹With respect to the direction of the exchanged virtual photon, the hard probe.

²More precisely, they are the only three leading-twist PDFs that survive integration over the parton momentum components that are transverse with respect to the direction of the hard probe.

tion (FF) [2]: the poorly known chiral-odd Collins function H_1^\perp , describing the correlation between the quark transverse spin and the transverse momentum of the produced hadron, or the relatively well known spin-independent chiral-even D_1 FF. Three of the eight TMDs are the transverse-momentum-dependent versions of f_1 , g_1 and h_1 . The other five are the Sivers function f_{1T}^\perp , the Boer-Mulders function h_1^\perp , the *pretzelosity* function h_{1T}^\perp and the so-called *worm-gear* functions h_{1L}^\perp and g_{1T}^\perp .

The HERMES experiment at HERA has played a pioneering role in these studies, by measuring observables (azimuthal asymmetries) sensitive to these (and also some higher-twist) TMDs, in some cases providing the first evidence of non-zero effects. Most of the HERMES results are confirmed by other experiments (COMPASS, CLAS, etc.), though intriguing differences were observed in some cases. High-precision results from the next generation high-luminosity and large-acceptance experiments (at present or upgraded facilities and, possibly, at the future Electron-Ion Collider) will greatly improve our understanding of the nucleon structure in terms of TMDs.

2.1 Transversity and Collins functions

The first evidence for a non-zero transversity function was reported by the HERMES Collaboration in 2005 [3]. HERMES measured significant asymmetry amplitudes (*Collins amplitudes*) in the production of π^+ and π^- in SIDIS, using an unpolarized 27.5 GeV electron beam and a transversely polarized hydrogen target. These amplitudes are sensitive to the convolution of the transversity function and the Collins FF (the so-called *Collins effect*), which causes the observed azimuthal distribution of the final-state hadrons (pions in this case) generated in the fragmentation of transversely polarized quarks:

$$A_{UT}^{\sin(\phi+\phi_S)} \propto \sum_q e_q^2 h_1^q(x, p_T^2) \otimes H_1^{\perp,q}(z, k_T^2). \quad (2.1)$$

Here, ϕ and ϕ_S are, respectively, the azimuthal angle of the detected hadron and of the target transverse polarization with respect to the lepton scattering plane and about the virtual-photon direction (see Fig. 1), z denotes the fraction of the energy of the exchanged virtual photon carried by the produced hadron (in this case a pion), and p_T and k_T represent the transverse momentum of the struck quark and that of the fragmenting quark, respectively.

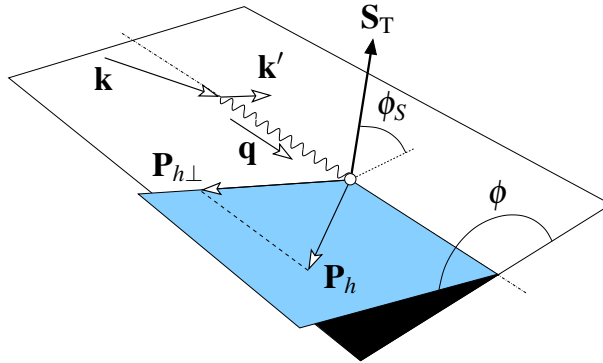


Figure 1: Schematic view of the SIDIS process with the description of the azimuthal angles ϕ and ϕ_S .

The measured Collins amplitudes for π^+ and π^- have similar magnitude and opposite sign. This unexpected result can be interpreted assuming that the scattering process involves predominantly the u quarks (u -quark dominance) and that the unfavored Collins function (responsible for the formation of a π^-) has approximately the same size and opposite sign of the favored one (responsible for the formation of a π^+): $H_{1,unfav}^{u \rightarrow \pi^-} \approx -H_{1,fav}^{u \rightarrow \pi^+}$. This hypothesis is consistent with the recent measurements of azimuthal asymmetries sensitive to the Collins function performed at the BELLE [4] and BABAR [5] experiments. A global analysis of the Collins amplitudes for pions measured at HERMES, together with the analogous results from the COMPASS experiment obtained using a transversely polarized deuteron target [6] and the azimuthal asymmetries measured in e^+e^- collisions from BELLE yielded the first extraction of the transversity function for u and d flavours and to be substantially smaller than the corresponding positivity bounds [7].

The final HERMES results [8], based on the full statistics available, confirm the main features of the early results for charged pions and include results for neutral pions and charged kaons. The amplitudes for K^+ are large and positive while those for π^0 and K^- are consistent with zero. The results, provided in 1-dimensional (1D) projections as a function of x , z or $P_{h\perp}$, are shown in Fig. 2. Recently, the data analysis was refined and the relevant asymmetry amplitudes were extracted in a 3-dimensional (3D) binning in x , z and $P_{h\perp}$. The 3D binning allows to map the kinematic dependence of the asymmetry amplitudes in a greatly detailed way. As an example, Fig. 3 shows the Collins amplitude for π^- as a function of x in simultaneous bins in z and $P_{h\perp}$. The rise in magnitude of the Collins amplitude for π^- as a function of x , as observed in the conventional 1D projection, reveals non-trivial kinematic dependencies in z and $P_{h\perp}$ when observed in the 3D representation, where most of the rise is clearly localized in the high- x and high- $P_{h\perp}$ region. Recently, the HERMES experiment has also measured single and double-spin asymmetries in SIDIS for protons and antiprotons. Figure 4 shows the Collins amplitudes for protons and antiprotons in 1D bins in x , z and $P_{h\perp}$. Both results are consistent with zero.

2.2 The Sivers function

Among the TMDs, particularly interesting is the Sivers function. It describes the correlation between the quark transverse momentum and the transverse spin of the nucleon. The interest in this TMD, proposed more than 20 years ago [9] to explain the large single-spin asymmetries observed in pion production in the collision of unpolarized with transversely polarized nucleons, suddenly increased after it was demonstrated [10] to be linked to the quark and gluon orbital angular momentum, the main still unmeasured contribution to the nucleon spin. It is naive-T-odd, i.e. it requires final-state interactions (FSIs) of the ejected quark with the color field of the nucleon remnant. These FSIs are formally introduced in the definition itself of the Sivers function through a gauge link. In general, gauge links are process-dependent and this leads to the remarkable fact that naive-T-odd TMDs (such as the Sivers and the Boer-Mulders functions) are not universal. In particular, they are expected to have opposite sign when measured in Drell-Yan processes. The experimental verification of this direct QCD prediction is eagerly awaited.

The first evidence for a non-zero Sivers function was reported by the HERMES Collaboration in 2005 [3], through the extraction of asymmetry amplitudes from data collected with an unpolar-

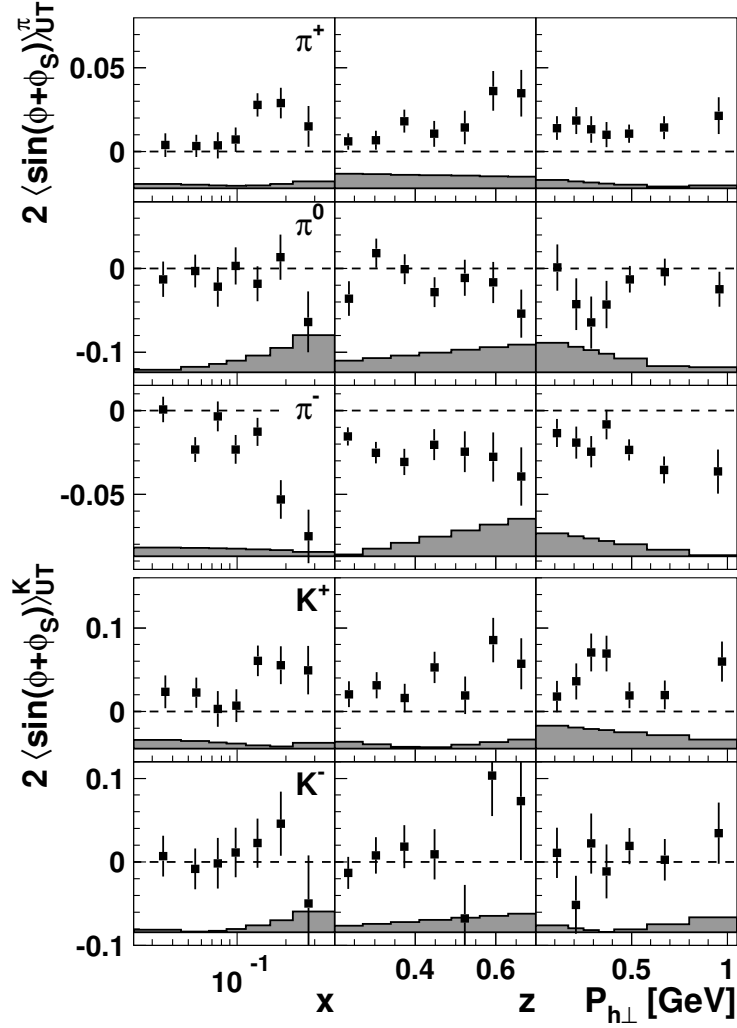


Figure 2: Collins amplitudes for pions and charged kaons as a function of x , z , and $P_{h\perp}$. A 7.3% scale uncertainty, not shown, arises from the accuracy in the measurement of the (transverse) target polarization.

ized 27.5 GeV electron beam and a transversely polarized hydrogen target. These amplitudes are sensitive to the convolution of the Sivers function f_{1T}^\perp and the unpolarized fragmentation function D_1 :

$$A_{UT}^{\sin(\phi - \phi_s)} \propto \sum_q e_q^2 f_{1T}^{\perp, q}(x, p_T^2) \otimes D_1^q(z, k_T^2). \quad (2.2)$$

In particular, HERMES observed large positive amplitudes for π^+ and amplitudes consistent with zero for π^- . The vanishing amplitudes for π^- require cancellation effects, e.g., from a d -quark Sivers function opposite in sign to the u -quark Sivers function. The final HERMES results [11] confirm the main features of the early results for charged pions and include results for neutral pions and charged kaons (Fig. 5). The amplitudes for K^+ are large and positive while those for π^0 and K^- are slightly positive. Unexpectedly, the K^+ amplitudes are larger than the π^+ ones.

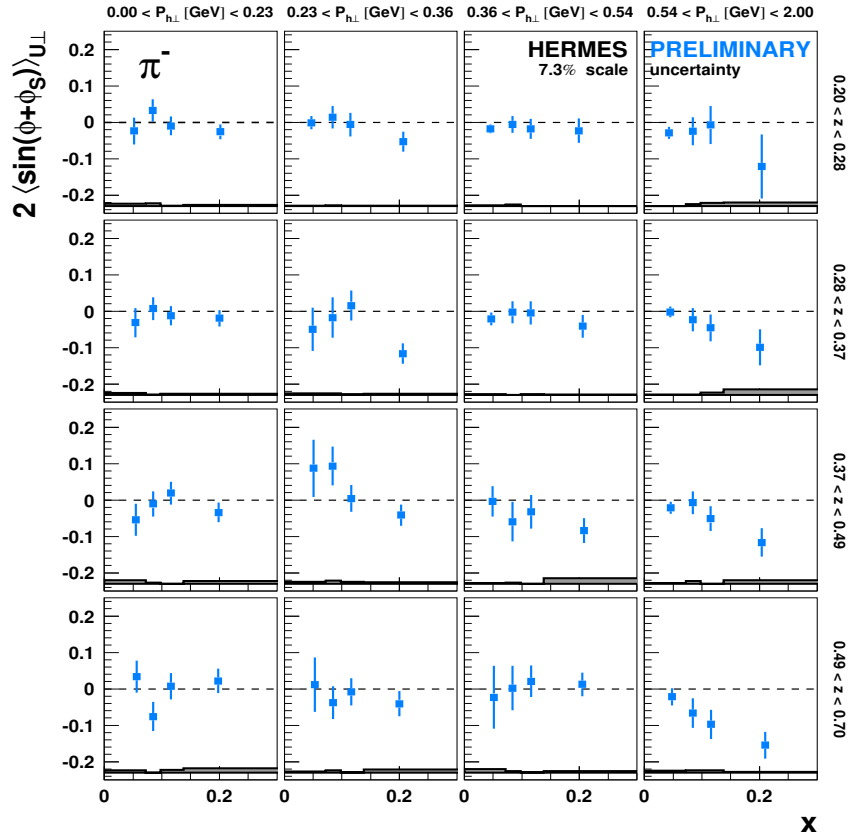


Figure 3: Collins amplitudes for π^- in 3-dimensional binning in x , z and $P_{h\perp}$.

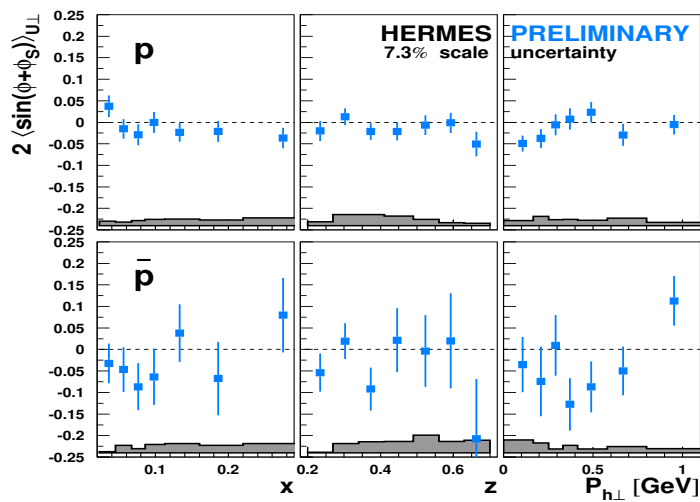


Figure 4: Collins amplitudes for protons and anti-protons as a function of x , z and $P_{h\perp}$.

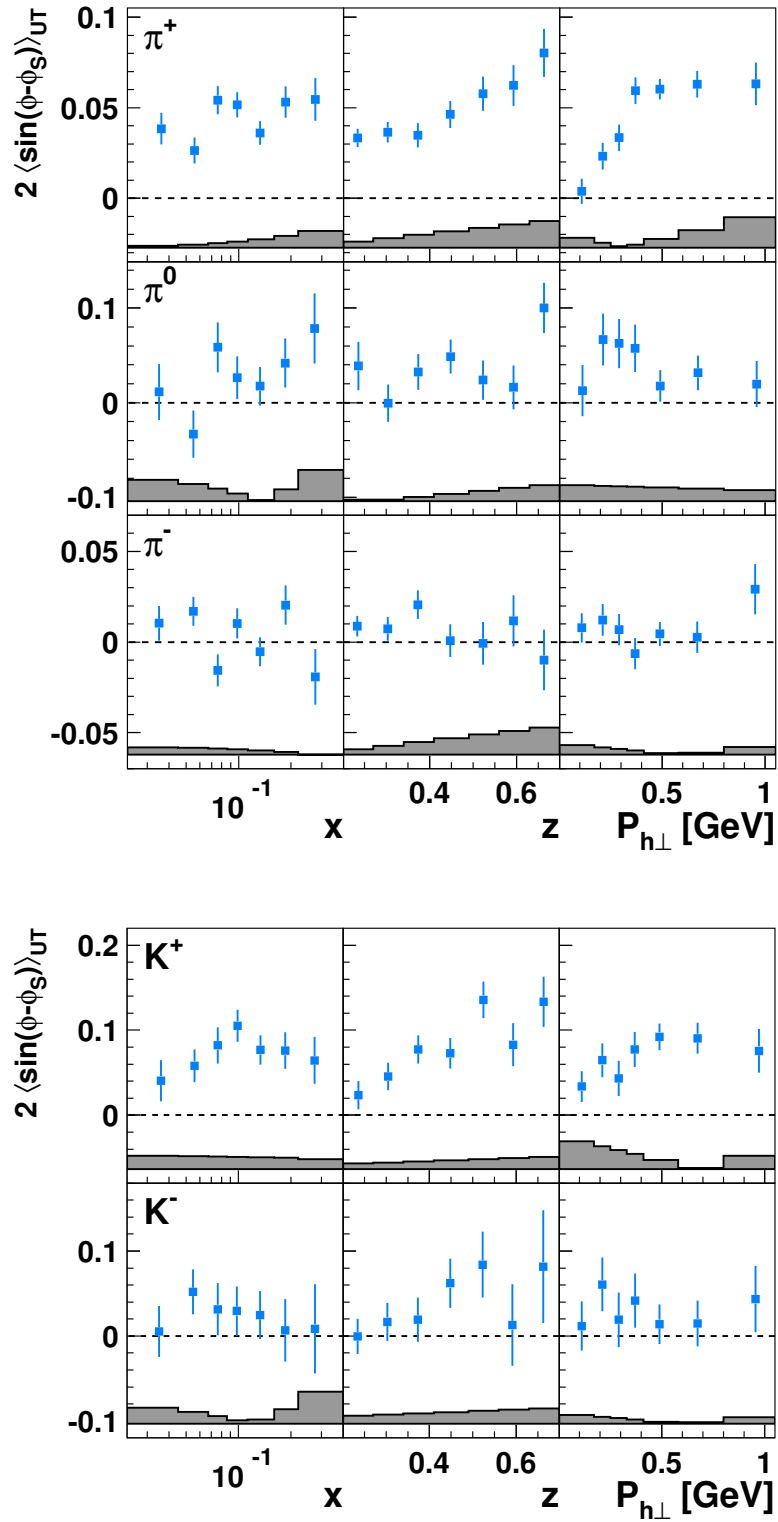


Figure 5: Sivers amplitudes for pions (top) and charged kaons (bottom) as a function of x , z , and $P_{h\perp}$. A 7.3% scale uncertainty, not shown, arises from the accuracy in the measurement of the (transverse) target polarization.

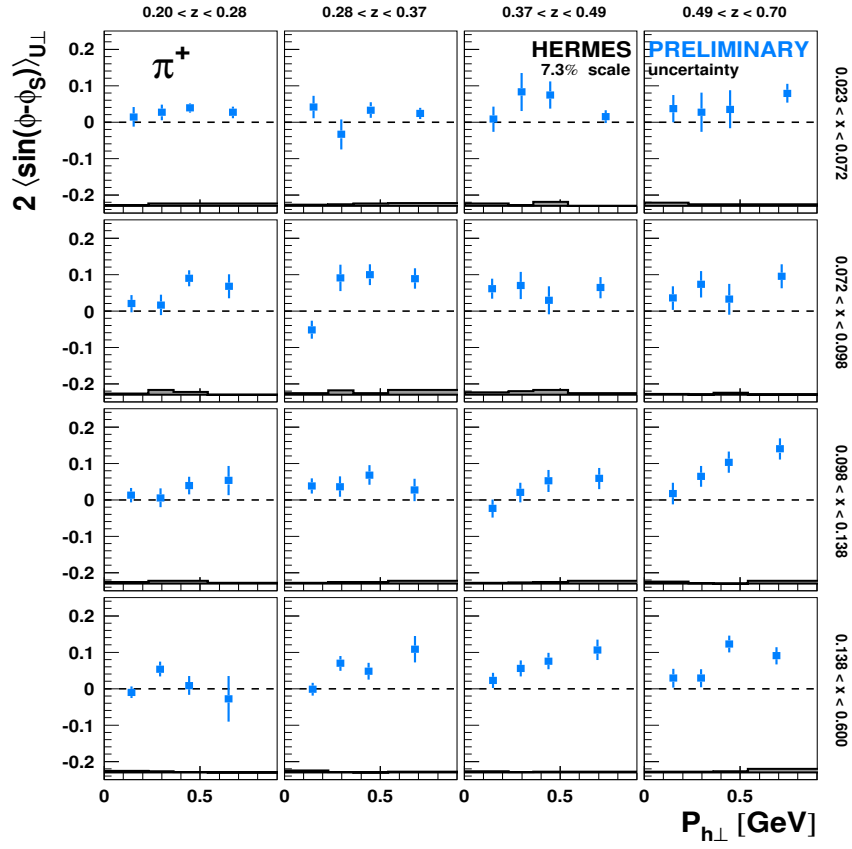


Figure 6: Sivers amplitudes for π^+ in 3-dimensional binning in x , z and $P_{h\perp}$.

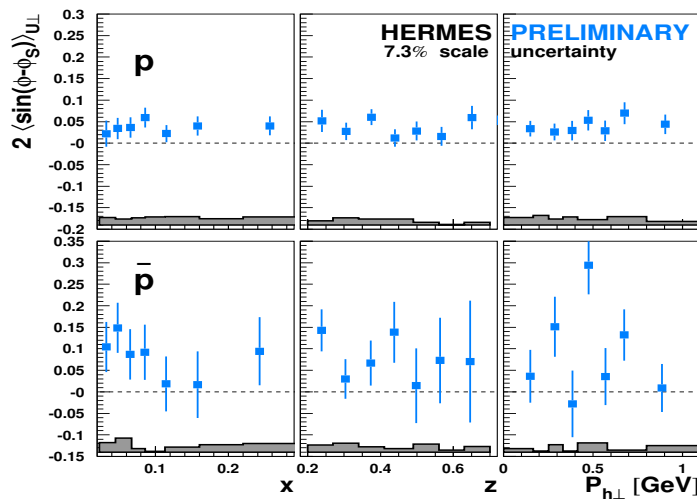


Figure 7: Sivers amplitudes for protons and anti-protons as a function of x , z and $P_{h\perp}$.

This observation can be ascribed, for instance, to a significant role of the sea quarks or to possible higher-twist contributions in kaon production. Figure 6 shows the Siverts amplitude for π^+ as a function of $P_{h\perp}$ in simultaneous bins in x and z . From the 3D representation it becomes clear that the rise of the Siverts amplitude for π^+ as a function of $P_{h\perp}$ is localized in the high- x and high- z region. Figure 7 shows the Siverts amplitudes for protons and antiprotons in 1D bins in x , z and $P_{h\perp}$. While the antiproton amplitude is consistent with zero within the experimental uncertainties, the proton data exhibit a small but significantly positive amplitude. This constitutes, at present, the first measurement of a non-zero Siverts effect for protons in SIDIS.

2.3 The Boer-Mulders function

Another very intriguing TMD is the Boer-Mulders function [12], describing the correlation between transverse polarization and transverse momentum of quarks in an unpolarized nucleon. Similarly to the Siverts function, it is naive-T-odd, i.e. in SIDIS it arises from final-state interactions of the ejected quark with the nucleon remnant. This feature is properly taken into account in the definition of the TMD through the introduction of a gauge link. Since it involves only the parton spin and not the nucleon spin, the Boer-Mulders mechanism is responsible for spin-related effects even in unpolarized reactions. In SIDIS the Boer-Mulders function, in combination with the Collins function, generates at leading twist a $\cos 2\phi$ azimuthal modulation of the unpolarized cross section:

$$d\sigma_{UU}(\phi) \propto \cos 2\phi \cdot \sum_q e_q^2 h_1^{\perp,q}(x, p_T^2) \otimes H_1^{\perp,q}(z, k_T^2) + \dots \quad (2.3)$$

At twist-three it also contributes to a $\cos\phi$ modulation together with the *Cahn effect*, a pure kinematic effect due to the transverse motion of partons in the nucleon.

The HERMES Collaboration has measured both cross-section modulations using unpolarized electron and positron beams and unpolarized hydrogen and deuterium targets [13]. The amplitudes are extracted separately for charged pions and kaons in a four-dimensional kinematic space spanned by x , y , z and $P_{h\perp}$, where y denotes the fraction of the beam energy carried by the virtual photon. The large $\cos 2\phi$ amplitudes measured for both pions and kaons constitute a clear evidence of a non-vanishing Boer-Mulders effect. In particular, the $\cos 2\phi$ amplitudes are of opposite sign for π^+ and π^- (Fig. 8) and of the same sign for K^+ and K^- (Fig. 9). In addition, the kaon amplitudes are significantly larger in magnitude than the pion ones, suggesting a possible substantial difference between the Collins FF for pions and kaons or a significant contribution to the Boer-Mulders effect from scattering off s quarks. In general, the results obtained with the hydrogen and the deuterium targets are very similar, suggesting a Boer-Mulders function of the same sign for u and d quarks (the opposite sign of the pion amplitudes can be ascribed to the opposite sign of the favored and unfavored Collins FFs). Concerning the higher-twist $\cos\phi$ modulation, the measured amplitudes are large and negative for π^+ , π^- and K^+ , while they are consistent with zero for K^- (Figs. 10 and 11). The similar x and y dependence of the $\cos\phi$ amplitude for π^+ and π^- suggests a weak flavour dependence of the Chan effect, while the remarkably different $P_{h\perp}$ dependence could arise from the flavour-dependent p_T dependence carried by the Boer-Mulders contribution to this harmonic. Finally, the substantial differences between the K^+ and the K^- results might be a consequence of poorly known interaction-dependent terms, also contributing to the $\cos\phi$ asymmetry.

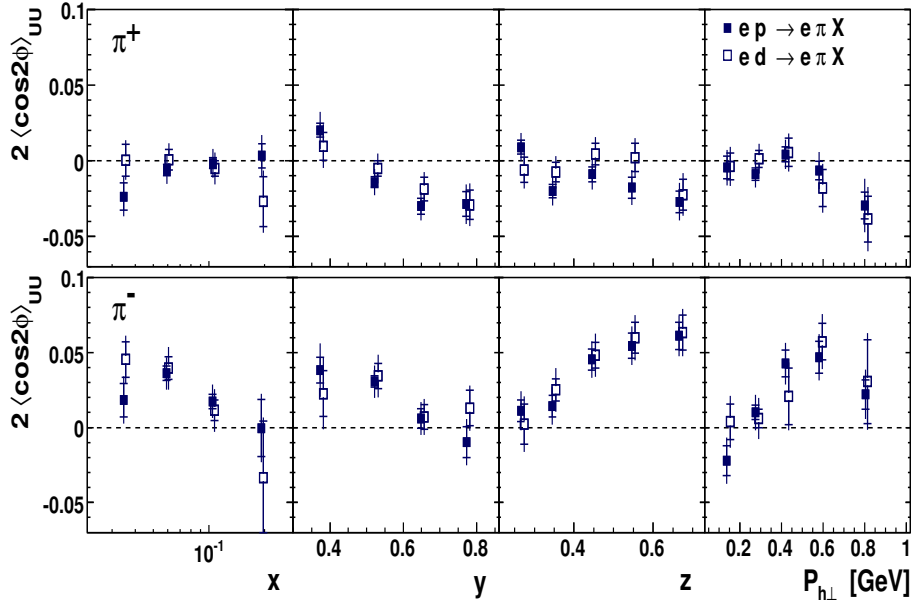


Figure 8: $\cos(2\phi)_{UU}$ asymmetry amplitudes for charged pions in 1D binning in x , y , z and $P_{h\perp}$.

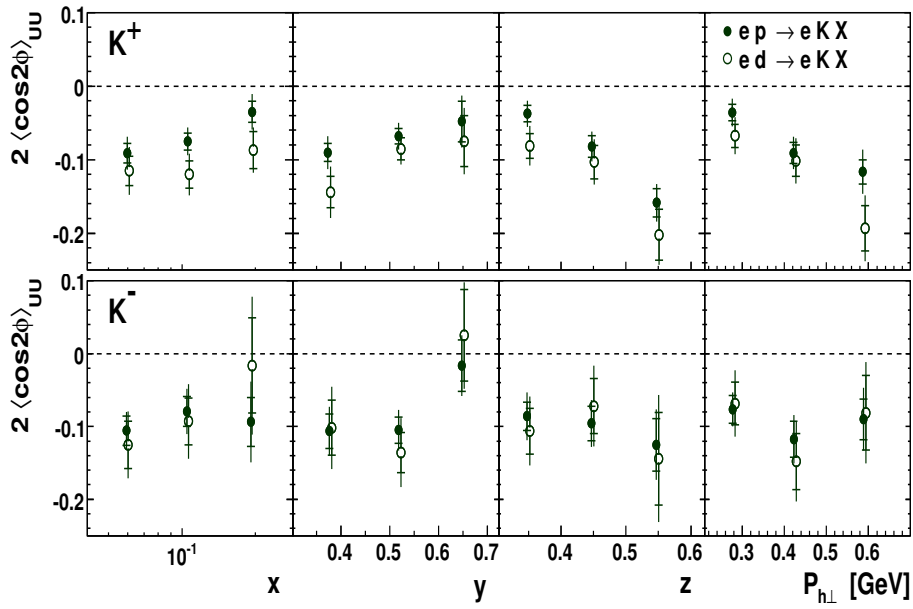


Figure 9: $\cos(2\phi)_{UU}$ asymmetry amplitudes for charged kaons in 1D binning in x , y , z and $P_{h\perp}$.

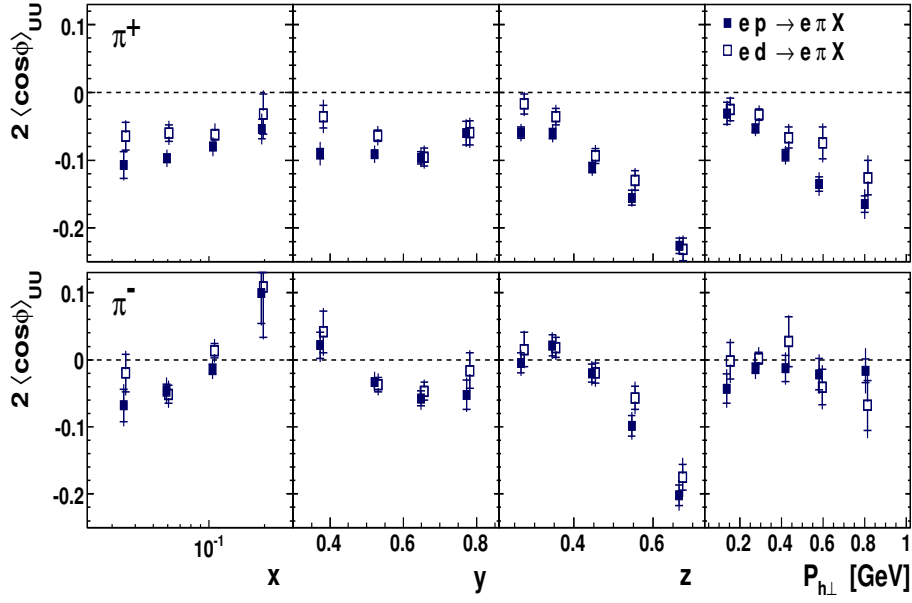


Figure 10: $\cos(\phi)_{UU}$ asymmetry amplitudes for charged pions in 1D binning in x , y , z and $P_{h\perp}$.

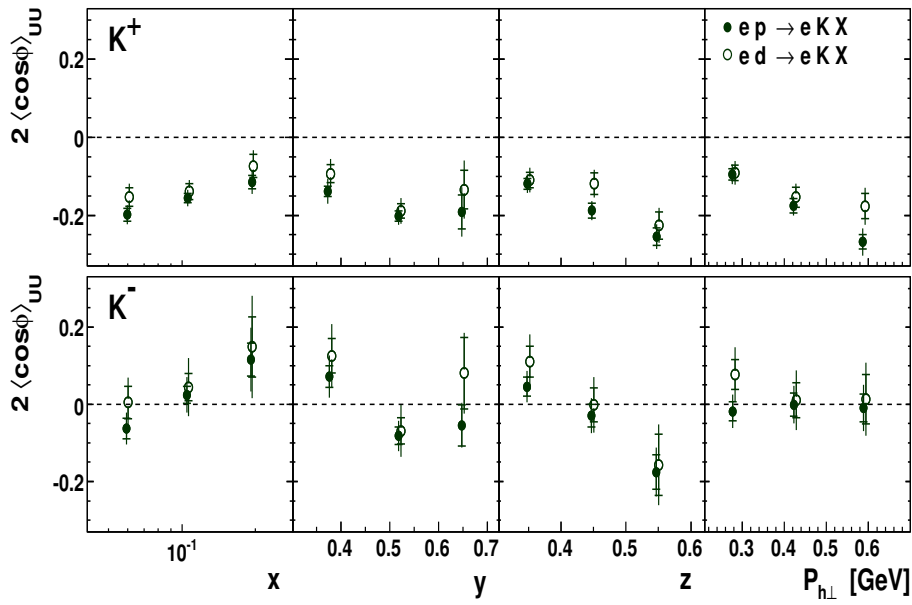


Figure 11: $\cos(\phi)_{UU}$ asymmetry amplitudes for charged kaons in 1D binning in x , y , z and $P_{h\perp}$.

3. Generalized Parton Distributions

The experimental access to GPDs is so far obtained from the measurements of hard exclusive lepton-nucleon scattering processes. These processes are described by four leading-twist, quark chirality conserving GPDs (H , E , \tilde{H} , and \tilde{E}). The cleanest process to probe GPDs is Deeply Virtual Compton Scattering (DVCS), $\ell + N \rightarrow \ell + N' + \gamma$, where a real photon is emitted by the struck quark in the nucleon. During the last decade the DVCS process was extensively studied both theoretically and experimentally. Currently there exist several measurements by HERMES, H1, ZEUS, CLAS and Hall-A experiments. The Bethe-Heitler (BH) process, where a real photon is radiated by the incoming or outgoing lepton, has the same initial and final state as the DVCS process. These two processes are thus experimentally indistinguishable, and therefore the total cross-section of hard lepto-production of real photons contains an interference term I , which depends on the charge of the lepton beam: $\sigma \propto |\mathcal{T}_{BH}|^2 + |\mathcal{T}_{DVCS}|^2 + I$. The individual terms of the cross-section can be decomposed into Fourier harmonics in the relevant azimuthal angles. Different Fourier components depend on different Compton Form Factors (CFFs), which in turn are convolutions of hard scattering amplitudes with the corresponding GPDs.

At HERMES, the DVCS process is accessed through measurements of cross-section asymmetries that appear in the azimuthal distributions of the final-state photons. Using data collected with longitudinally polarized electron and positron beams and unpolarized, longitudinally and transversely polarized hydrogen and deuterium targets, it was possible to measure asymmetries with respect to beam charge, beam polarization and target polarization alone and also with respect to their different combinations. An overview of all extracted azimuthal asymmetry amplitudes corresponding to the entire HERMES kinematics is presented in Fig. 12 for both hydrogen and deuterium targets. The amplitudes of the beam-helicity and beam-charge asymmetries $A_{LU,DVCS}(\phi)$, $A_{LU,I}(\phi)$ and $A_C(\phi)$ are presented in the top panels. Significant non-zero $\cos(\phi)$ and $\sin(\phi)$ amplitudes are observed respectively for the beam-charge $A_C(\phi)$ and beam-helicity $A_{LU,I}(\phi)$ asymmetries. The results for the $\sin(\phi)$ amplitude of the charge-averaged beam-helicity asymmetry $A_{LU,DVCS}(\phi)$ are consistent with zero. In the bottom panels, the results of the longitudinal single-target-spin $A_{UL}(\phi)$ and double-spin $A_{LL}(\phi)$ asymmetries are presented. Also shown are the leading amplitudes of transverse single-target-spin and double-spin asymmetries, measured on hydrogen target. The amplitudes $A_{UT,I}^{\sin(\phi-\phi_S)\cos(\phi)}$ and $A_{LT,I}^{\sin(\phi-\phi_S)\sin(\phi)}$ are significantly negative and consistent with zero, respectively. Full references for the HERMES DVCS results on hydrogen and deuterium targets can be found in [14, 15, 16, 17, 18, 19, 20]. At Hermes, DVCS studies were also performed for the first time on heavier nuclear targets, ranging from He to Xe [21]. The resulting beam-charge and beam-helicity asymmetries were found to be consistent with those on a free proton target and no nuclear-mass dependence was observed.

Apart from DVCS, complementary information on GPDs can be obtained from measurements of hard exclusive meson production processes $\ell + N \rightarrow \ell + N' + V$. Unlike DVCS, the situation with hard meson production is in a less advanced stage. First of all the factorisation is not proven for all the amplitudes, thus the interpretation of the observations in terms of GPDs requires more sophisticated measurements with possible separation of different amplitudes. In addition, a good knowledge of meson distribution amplitudes is required. On the other side, measurements of exclusive meson production processes with different final state mesons (ρ , ϕ , ω , etc.) provide a unique

opportunity to study the flavour dependence of GPDs. As an example, Fig. 13 shows the complete set of Spin Density Matrix Elements (SDMEs) for exclusively produced ρ and ϕ mesons, obtained using unpolarized and longitudinally polarized hydrogen and deuterium targets. Full references for the HERMES SDMEs measurements can be found in [22, 23, 24].

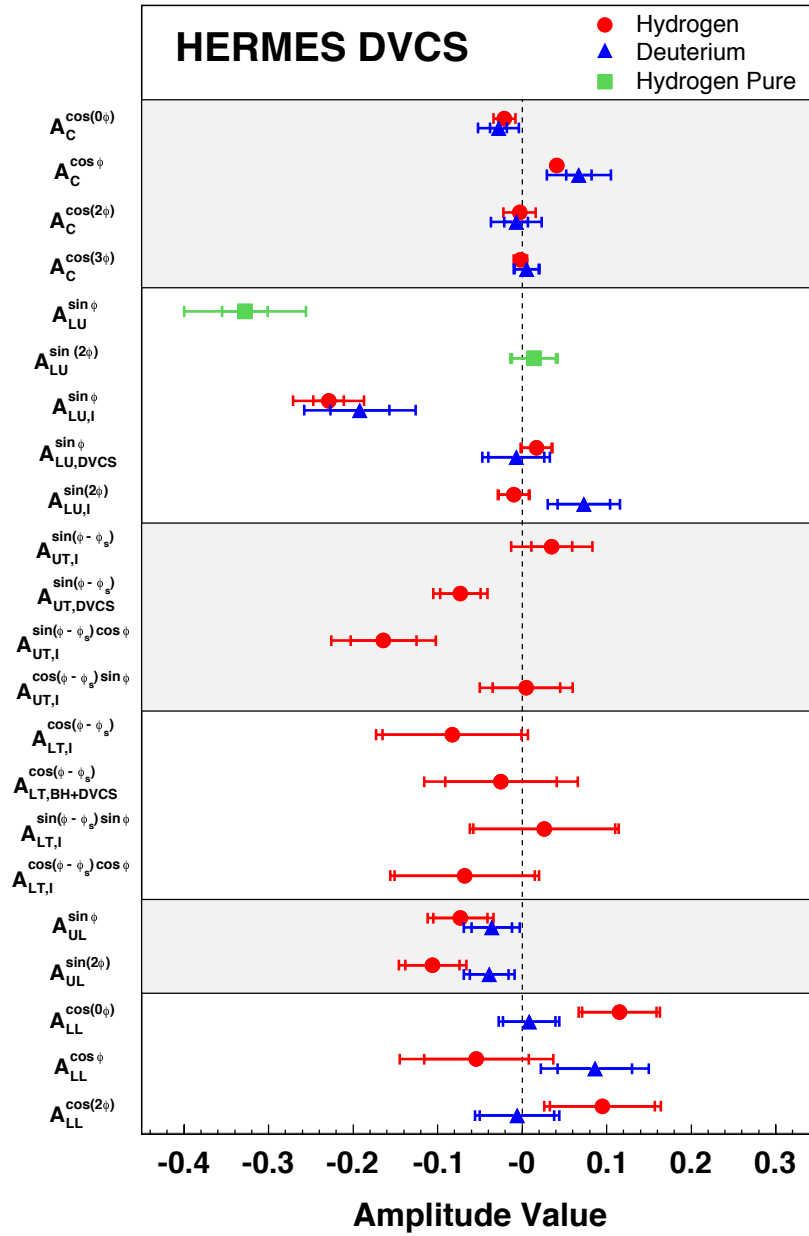


Figure 12: Overview of DVCS amplitudes measured over the entire HERMES kinematic range.

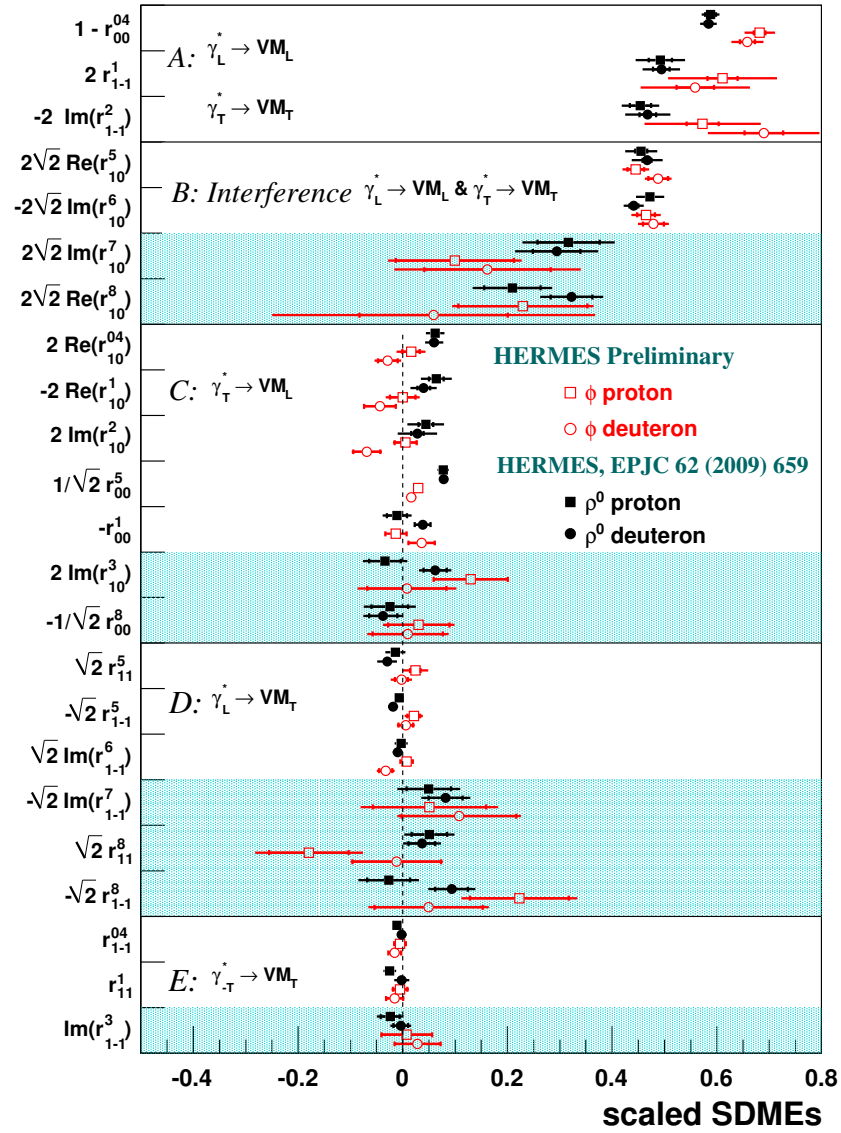


Figure 13: Overview of ρ and ϕ SDMEs measured on both proton and deuteron targets over the entire HERMES kinematic range.

4. Summary

The study of the three-dimensional structure of nucleons in terms of TMDs and GPDs is a relatively young and fast evolving field. A rich phenomenology arises when the transverse degrees of freedom (spin, momentum, location) of quarks and gluons, for long time neglected, are not integrated out. HERMES, as a pioneering experiment, has played a key exploratory role in this field. New precision data from present and future experiments, operating in complementary kinematic domains, will push forward our present understanding of the nucleon structure and will allow to map the phase-space distributions of quarks and gluons with unprecedented precision.

References

- [1] K. A. Olive *et al.* (PDG), *Chin. Phys. C* **38**, 090001 (2014).
- [2] A. Bacchetta *et al.*, *JHEP* **02**, 093 (2007).
- [3] A. Airapetian *et al.* (HERMES), *Phys. Rev. Lett.* **94**, 012002 (2005).
- [4] R. Seidl *et al.* (BELLE), *Phys. Rev. D* **78**, 032011 (2008), *Phys. Rev. D* **86**, 039905 (2012).
- [5] J. P. Lees *et al.* (BABAR), *Phys. Rev. D* **90**, 052003 (2014).
- [6] E. S. Ageev *et al.* (COMPASS), *Nucl. Phys. B* **765**, 31 (2007).
- [7] M. Anselmino *et al.*, *Phys. Rev. D* **75**, 054032 (2007).
- [8] A. Airapetian *et al.* (HERMES), *Phys. Lett. B* **693**, 11 (2010).
- [9] D. W. Sivers, *Phys. Rev. D* **41**, 83 (1990).
- [10] S. J. Brodsky *et al.* *Phys. Lett. B* **530**, 99 (2002).
- [11] A. Airapetian *et al.* (HERMES), *Phys. Rev. Lett.* **103**, 152002 (2009).
- [12] A. Airapetian *et al.* (HERMES), *Phys. Rev. D* **57**, 5780 (1998).
- [13] A. Airapetian *et al.* (HERMES), *Phys. Rev. D* **87**, 012010 (2013).
- [14] A. Airapetian *et al.* (HERMES), *JHEP* **07**, 032 (2012).
- [15] A. Airapetian *et al.* (HERMES), *JHEP* **06**, 019 (2010).
- [16] A. Airapetian *et al.* (HERMES), *JHEP* **06**, 066 (2008)
- [17] A. Airapetian *et al.* (HERMES), *Phys. Lett. B* **704**, 15 (2011).
- [18] A. Airapetian *et al.* (HERMES), *Nucl. Phys. B* **829**, 1 (2010).
- [19] A. Airapetian *et al.* (HERMES), *Nucl. Phys. B* **842**, 265 (2011).
- [20] A. Airapetian *et al.* (HERMES), *JHEP* **10**, 042 (2012).
- [21] A. Airapetian *et al.* (HERMES), *Phys. Rev. C* **81**, 035202 (2010).
- [22] A. Airapetian *et al.* (HERMES), *Eur. Phys. J. C* **62**, 659 (2009).
- [23] A. Airapetian *et al.* (HERMES), *Eur. Phys. J. C* **74**, 3110 (2014).
- [24] A. Airapetian *et al.* (HERMES), *Phys. Lett. B* **679**, 100 (2009).